

Verified Compositions of Neural Network Controllers for Temporal Logic Control Objectives

Jun Wang, Samarth Kalluraya and Yiannis Kantaros

Abstract—This paper presents a new approach to design verified compositions of Neural Network (NN) controllers for autonomous systems with tasks captured by Linear Temporal Logic (LTL) formulas. Particularly, the LTL formula requires the system to reach and avoid certain regions in a temporal/logical order. We assume that the system is equipped with a finite set of trained NN controllers. Each controller has been trained so that it can drive the system towards a specific region of interest while avoiding others. Our goal is to check if there exists a temporal composition of the trained NN controllers - and if so, to compute it - that will yield composite system behaviors that satisfy a user-specified LTL task for any initial system state belonging to a given set. To address this problem, we propose a new approach that relies on a novel integration of automata theory and recently proposed reachability analysis tools for NN-controlled systems. We note that the proposed method can be applied to other controllers, not necessarily modeled by NNs, by appropriate selection of the reachability analysis tool. We focus on NN controllers due to their lack of robustness. The proposed method is demonstrated on navigation tasks for aerial vehicles.

I. INTRODUCTION

Several methods have been proposed recently to train Neural Network (NN) controllers for autonomous systems. Such training methods include e.g., deep reinforcement learning (RL) [1] and model predictive control (MPC) [2]. Despite the high real-time performance of NN-driven systems, they typically lack safety and robustness guarantees as underscored by recent studies [3]. To address this limitation, various methods have been proposed to verify robustness properties of trained NN controllers [4], [5]. For instance, [5] addresses the problem of output range analysis of trained NNs given an input set. Safety verification of dynamical systems with feedback NN controllers has been studied as well in [6]–[12] and the references therein. Typically, these methods investigate if a dynamical system with a trained NN controller can satisfy a reach-avoid property given a set of possible initial states.

Common in all the above works is that they focus on learning or verifying the efficiency/safety of a *single* NN controller for a given task. However, the sample complexity and computational cost of learning a *single* NN controller increases drastically as the task complexity increases. Motivated by these limitations, compositional RL methods have been proposed recently that aim to learn a set of base NN controllers which are then composed to satisfy a complex task captured by temporal logics; see e.g., [13]–[15]. The

key idea in these works is to decompose the task into simpler sub-tasks for which NN controllers can be learned, using RL, more efficiently. Then, these NN controllers are composed to satisfy the original task. Nevertheless, the resulting controllers often either lack safety guarantees or the provided guarantees are impractical (e.g., lower bounds on satisfaction probability) for safety-critical applications; also, these guarantees are typically specific to a fixed and given initial system state. To address this issue, in this paper we propose a new method to design *verified* temporal compositions of trained NN controllers for temporal logic tasks. Related is also the recent work in [16] which, however, unlike the above papers and ours, does not consider temporal logic tasks. For instance, in [16], the sub-tasks are revealed by the environment while in [13]–[15] the sub-tasks are ‘strategically’ selected to satisfy a temporal logic task.

Specifically, in this paper, we consider autonomous systems tasked with complex high-level missions captured by a fragment of Linear Temporal Logic (LTL), called co-safe LTL [17]. We assume that the system is governed by discrete-time linear time-varying dynamics and that the LTL task requires reaching and avoiding certain regions in a temporal/logical order. Also, the system has access to a finite set of already trained controllers modeled as NNs. Each controller is trained so that it can drive the system towards a specific region of interest while avoiding others. We do not make any assumptions about how these NNs have been trained; for instance they may have been trained using RL or MPC-based methods. Our goal is to check if there exists a temporal composition of these NN controllers - and if so, to compute it - that will yield composite system behaviors that always satisfy a user-specified LTL task for any initial system state belonging to a given set. To address this problem, we leverage automaton representations of LTL formulas as well as graph-search methods and existing reachability analysis for NN-driven systems [8]. We note that our approach can handle any other open-loop or feedback controllers that are not necessarily modeled as NNs by appropriate selection of the reachability analysis method. In this paper we focus on NN controllers due to their fragility to imperceptible input perturbations [3].

Contributions: *First*, we propose a new approach to design verified temporal compositions of NN controllers for co-safe LTL tasks. *Second*, we show correctness of the proposed method and discuss trade-offs between completeness and computational efficiency. *Third*, we demonstrate the efficiency of the proposed approach on several navigation tasks that involve aerial vehicles.

The authors are with the Department of Electrical and Systems Engineering, Washington University in St. Louis, St. Louis, MO. Email: {junw, k.samarth, ioannisk}@wustl.edu

II. PROBLEM FORMULATION

Closed-loop system: We consider discrete-time linear systems defined as follows:

$$\mathbf{x}_{t+1} = \mathbf{f}(\mathbf{x}_t, \mathbf{u}_t) = \mathbf{A}_t \mathbf{x}_t + \mathbf{B}_t \mathbf{u}_t + \mathbf{c}_t, \quad (1)$$

where $\mathbf{x}_t \in \mathcal{X} \subseteq \mathbb{R}^d$ and $\mathbf{u}_t \in \mathcal{U}_t \subseteq \mathbb{R}^n$ denote the state and the control input of the system at time $t \geq 0$, respectively. Also, $\mathbf{A}_t \in \mathbb{R}^{d \times d}$, $\mathbf{B}_t \in \mathbb{R}^{d \times n}$ are the system matrices while $\mathbf{c}_t \in \mathbb{R}^d$ is an exogenous input. We assume that state-space \mathcal{X} contains $N > 0$ sub-spaces denoted by $\ell_i \subset \mathcal{X}$ modelling regions of interest or unsafe areas. Also, we assume that at any time t the system can apply control inputs selected from a finite set of feedback controllers collected in the set $\Xi = \{\xi_i\}_{i=1}^N$, where $\xi_i(\mathbf{x}_t) : \mathcal{X} \rightarrow \mathbb{R}^n$ maps system states to control actions. We assume that the controller ξ_i is selected by the system when, given any initial state in \mathcal{X} , the system state \mathbf{x}_t needs to be driven towards the interior of ℓ_i . We consider cases where the controllers $\xi_i(\mathbf{x}_t)$ are parameterized by multi-layer feed-forward fully-connected neural networks (NNs). Such NN controllers can be implemented using available methods; see e.g., [18]. Hereafter, with slight abuse of notation, we denote by $\xi(t)$ the controller selected from Ξ at time t . To ensure that NN output respects the input constraint, we consider a projection operator, denoted by $\text{Proj}_{\mathcal{U}_t}$, and define the control input as $\mathbf{u}_t = \text{Proj}_{\mathcal{U}_t} \xi(t)$. We denote the closed-loop system with dynamics (1) and the projected NN control policy as:

$$\mathbf{x}_{t+1} = \mathbf{f}_\xi(\mathbf{x}_t) \quad (2)$$

Next, we define a high-level NN-based control strategy ξ as a *temporal composition* of the controllers in Ξ .

Definition 2.1 (Control Strategy): A NN-based control strategy ξ is defined as a finite sequence of NN controllers selected from Ξ , i.e., $\xi = \mu(0), \mu(1), \mu(2), \dots, \mu(K)$, for some finite $K > 0$, where $\mu(k) \in \Xi$, for all $k \in \{0, 1, \dots, K\}$, and $\mu(k)$ is applied for a finite horizon H_k .

We note again that $\mu(k)$ is a feedback controller from Ξ . For instance, if $\mu(0) = \xi_i$, for some $i \in \{1, \dots, N\}$, then the system applies the controller $\xi_i(\mathbf{x}_t)$, $\forall t \in \{0, 1, \dots, H_0\}$. Given ξ and an initial state \mathbf{x}_0 , the corresponding closed-loop system (2) generates a finite sequence of system states, denoted by $\tau(\mathbf{x}_0) = \mathbf{x}_0, \mathbf{x}_1, \dots, \mathbf{x}_t, \dots, \mathbf{x}_F$, where $F = \sum_{k=0}^K H_k$.

Linear Temporal Logic Properties: We define mission and safety properties for the system (1) using Linear Temporal Logic (LTL) as it allows to specify a wide range of high-level tasks [19], [20]. LTL consists of atomic propositions (i.e., Boolean variables), denoted by \mathcal{AP} , Boolean operators, (i.e., conjunction \wedge , and negation \neg), and two temporal operators, next \bigcirc and until \mathcal{U} . LTL formulas over a set \mathcal{AP} can be constructed based on the following grammar: $\phi ::= \text{true} \mid \pi \mid \phi_1 \wedge \phi_2 \mid \neg \phi \mid \bigcirc \phi \mid \phi_1 \mathcal{U} \phi_2$, where $\pi \in \mathcal{AP}$. For brevity we abstain from presenting the derivations of other Boolean and temporal operators, e.g., *always* \square , *eventually* \diamond , *implication* \Rightarrow , which can be found in [17]. Hereafter, we define the set \mathcal{AP} as $\mathcal{AP} = \cup_i \{\pi^{\ell_i}\}$,

where π^{ℓ_i} is an atomic predicate that is true when the system state \mathbf{x}_t is within region ℓ_i . We restrict our attention to co-safe LTL properties that exclude the use of the ‘always’ operator. Co-safe LTL formulas are satisfied by discrete finite plans τ defined as finite sequences of system states $\mathbf{x}_t \in \mathcal{X}$. i.e., $\tau(\mathbf{x}_0) = \mathbf{x}_0, \mathbf{x}_1, \dots, \mathbf{x}_t, \dots, \mathbf{x}_F$, where $F > 0$ denotes a finite horizon [17]. Given ξ and an initial state \mathbf{x}_0 , we say that the closed-loop system (2) satisfies ϕ , denoted by $\mathbf{f}_\xi \models \phi$, if (2) generates a sequence $\tau(\mathbf{x}_0)$ that satisfies ϕ .

Example 2.2: Examples of co-safe LTL specifications follow: (i) $\phi = \diamond(\pi^{\ell_1}) \wedge (\neg \pi^{\ell_2} \mathcal{U} \pi^{\ell_1})$ captures a common reach-avoid property requiring the system to eventually reach the region of interest ℓ_1 while avoiding in the meantime the unsafe region ℓ_2 ; (ii) $\phi = (\diamond \pi^{\ell_1}) \wedge (\diamond \pi^{\ell_2}) \wedge (\diamond \pi^{\ell_3}) \wedge (\diamond \pi^{\ell_4}) \wedge (\neg \pi^{\ell_4} \mathcal{U} \pi^{\ell_1})$ requires the system to eventually reach the regions ℓ_1, ℓ_2, ℓ_3 , and ℓ_4 , in any order, as long as ℓ_4 is avoided until region ℓ_1 is reached.

Problem 1: Given (i) a set of initial states $\mathcal{X}_0 \subseteq \mathcal{X}$; (ii) the system dynamics (1); (iii) a co-safe LTL property ϕ ; and (iv) a finite set Ξ of NN controllers, check if there exists a NN-based control strategy ξ (Definition 2.1), so that $\mathbf{f}_\xi \models \phi$, for all $\mathbf{x}_0 \in \mathcal{X}_0$; if there exists such a ξ , compute it as well.

Remark 2.3 (Controllers for LTL tasks): Several reinforcement learning (RL) methods have been proposed that can train a *single* controller, that can be parameterized by a NN, to satisfy an LTL task ϕ ; see e.g., [1], [21]–[23] and the references therein. Verification of a single NN controller (as opposed to the set of controllers considered here) with respect to an LTL formula can be accomplished by existing reachability analysis tools for discrete-time systems; see e.g., [8]. Particularly, a sequence of reachable sets, capturing all possible system states at future time instants t , needs to be computed under the considered NN controller and a set of initial states \mathcal{X}_0 . Then, it suffices to check if the atomic predicates that are satisfied across this sequence construct a word that can be accepted by an automaton of ϕ [17].

III. VERIFIED COMPOSITIONS OF NN CONTROLLERS FOR CO-SAFE LTL TASKS

Our approach to solve Problem 1 consists of the following steps. First, we translate the LTL formula ϕ into a Deterministic Finite state Automaton (DFA); see Section III-A. Second, by leveraging the DFA, we decompose ϕ into reach-avoid sub-tasks; see Sections III-B-III-C. Then, we apply graph-search methods combined with reachability analysis to check if there exists ξ so that $\mathbf{f}_\xi \models \phi$, for all $\mathbf{x}_0 \in \mathcal{X}_0$; see Section III-D. Trade-offs between completeness and computational efficiency are discussed in Section III-E.

A. From LTL formulas to DFA

First, we translate ϕ , constructed using \mathcal{AP} , into a DFA defined as follows [17]; see also Fig. 1a.

Definition 3.1 (DFA): A Deterministic Finite state Automaton (DFA) D over $\Sigma = 2^{\mathcal{AP}}$ is defined as a tuple $D = (\mathcal{Q}_D, q_D^0, \Sigma, \delta_D, q_D^F)$, where \mathcal{Q}_D is the set of states, $q_D^0 \in \mathcal{Q}_D$ is the initial state, Σ is an alphabet, $\delta_D : \mathcal{Q}_D \times \Sigma \rightarrow \mathcal{Q}_D$ is a deterministic transition relation, and $q_D^F \in \mathcal{Q}_D$ is the accepting/final state.

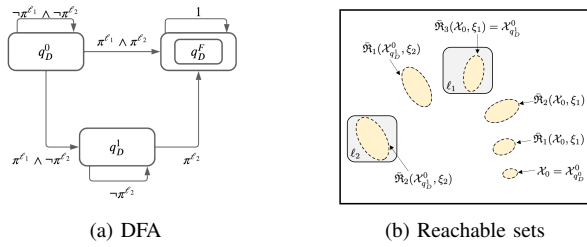


Fig. 1: Fig 1a shows the DFA corresponding to $\phi = \diamond(\pi^{\ell_2}) \wedge (\neg\pi^{\ell_2} \cup \pi^{\ell_1})$. Fig. 1b illustrates the reachability analysis over the DFA state space (see Section III-D).

To interpret a temporal logic formula over a sequence $\tau(\mathbf{x}_0)$ generated by (2), we use a labeling function $L : \mathcal{X} \rightarrow 2^{\mathcal{A}^P}$ that maps system states to symbols $\sigma \in 2^{\mathcal{A}^P}$. A finite sequence of states $\tau(\mathbf{x}_0) = \mathbf{x}_0, \mathbf{x}_1, \dots, \mathbf{x}_F$ satisfies ϕ if the word $w = L(\mathbf{x}_0)L(\mathbf{x}_1) \dots L(\mathbf{x}_F)$ yields an accepting DFA run, i.e., if starting from the initial state q_D^0 , each element in w yields a DFA transition so that the final state q_D^F is reached [17]. Note that a DFA can be constructed using existing tools such as [24].

B. From DFA to Reach-Avoid Properties

Given any DFA state $q_D \in \mathcal{Q}_D$, we compute a set \mathcal{R}_{q_D} that collects all DFA states that can be reached, in one hop, from q_D using a symbol σ . In math, we have:

$$\mathcal{R}_{q_D} = \{q'_D \mid q'_D = \delta_D(q_D, \sigma), \sigma \in \Sigma\}. \quad (3)$$

Then, given q_D and for each DFA state $q'_D \in \mathcal{R}_{q_D}$, we introduce the following definitions. We construct a set that collects the states $\mathbf{x} \in \mathcal{X}$, so that if the system state coincides with one of these states, then a symbol $\sigma = L(\mathbf{x}) \in \Sigma$ enabling this DFA transition will be generated. We collect these states in the set $\mathcal{X}_{q_D \rightarrow q'_D}$, i.e.,

$$\mathcal{X}_{q_D \rightarrow q'_D} = \{\mathbf{x} \in \mathcal{X} \mid q'_D = \delta_D(q_D, L(\mathbf{x}))\} \quad (4)$$

In what follows, for simplicity, we assume that for all $q_D \in \mathcal{Q}_D$ there exists a feasible self-loop around every DFA state q_D ; later, in Section III-C, we relax this assumption. Starting from any system state $\mathbf{x} \in \mathcal{X}$ and a DFA state q_D , transition from q_D to $q'_D \in \mathcal{R}_{q_D} \setminus q_D$ will eventually occur after $H_{q_D} \geq 0$ discrete time steps, if (i) the system state \mathbf{x}_t remains within $\mathcal{X}_{q_D \rightarrow q_D}$ for the next $H_{q_D} - 1$ steps, and (ii) at time $t = H_{q_D}$, we have that $\mathbf{x}_{H_{q_D}} \in \mathcal{X}_{q_D \rightarrow q'_D}$. Essentially, (i)-(ii) model a *reach-avoid* requirement. For instance, (i) may require a robot to stay within the obstacle-free space and (ii) may require a robot to eventually enter a region.

Example 3.2 (Reach-Avoid Properties): Consider the DFA in Fig. 1a. We have that $\mathcal{R}_{q_D^0} = \{q_D^0, q_D^1, q_D^F\}$. Also, we have that $\mathcal{X}_{q_D^0 \rightarrow q_D^0} = \mathcal{X} \setminus (\ell_1 \cup \ell_2)$, $\mathcal{X}_{q_D^0 \rightarrow q_D^1} = (\mathcal{X} \setminus \ell_2) \cap \ell_1$, $\mathcal{X}_{q_D^0 \rightarrow q_D^F} = \ell_2 \cap \ell_1$. Similarly, we have that $\mathcal{R}_{q_D^1} = \{q_D^1, q_D^F\}$, $\mathcal{X}_{q_D^1 \rightarrow q_D^1} = \mathcal{X} \setminus \ell_2$, and $\mathcal{X}_{q_D^1 \rightarrow q_D^F} = \ell_2$.

C. Verifying Reach-Avoid Properties

In what follows, we discuss how to check whether a transition from a DFA state q_D to $q'_D \neq q_D$ can be enabled; later, we will discuss how this can be used to verify LTL properties. Specifically, we want to verify that given an initial set of system states associated with q_D , denoted

by $\mathcal{X}_{q_D}^0$, the previously discussed conditions (i)-(ii) can be satisfied; the detailed construction of $\mathcal{X}_{q_D}^0$ will be discussed in Section III-D. Notice $\mathcal{X}_{q_D \rightarrow q'_D}$ may contain more than one region of interest ℓ_i . As discussed in Section II, for each region of interest ℓ_i in $\mathcal{X}_{q_D \rightarrow q'_D}$, the system selects the corresponding NN controller $\xi_i \in \Xi$. Hereafter, we collect all NN controllers associated with $\mathcal{X}_{q_D \rightarrow q'_D}$ in a set denoted by $\Xi_{q_D \rightarrow q'_D} \subseteq \Xi$.¹ In math, we want to show that there exists a finite horizon H_{q_D} and at least one NN controller $\xi \in \Xi_{q_D \rightarrow q'_D}$, so that if the system evolves as per $\mathbf{x}_{t+1} = \mathbf{f}(\mathbf{x}_t, \xi)$ then the following two conditions hold for all possible initial system states in $\mathcal{X}_{q_D}^0$: (i) $\mathbf{x}_t \in \mathcal{X}_{q_D \rightarrow q_D}, \forall t \in [0, H_{q_D} - 1]$ and (ii) $\mathbf{x}_{H_{q_D}} \in \mathcal{X}_{q_D \rightarrow q'_D}$. If such a horizon H_{q_D} and controller $\xi \in \Xi_{q_D \rightarrow q'_D}$ exist, then by definition of the set $\mathcal{X}_{q_D \rightarrow q'_D}$ in (4), we have that within the time interval $[0, H_{q_D} - 1]$, the transition from q_D to q_D (self-loop) is enabled, and at the time step $t = H_{q_D}$ the transition from q_D to q'_D occurs. In this case, we say that the DFA transition from q_D to q'_D is *verified to be safe* when the system starts anywhere within $\mathcal{X}_{q_D}^0$ and applies the NN controller ξ .

To reason about safety of a DFA transition, we leverage existing reachability analysis tools that can compute forward reachable sets $\mathfrak{R}_t(\mathcal{X}_{q_D}^0, \xi)$ collecting all possible states \mathbf{x} that the system may reach after applying a feedback NN controller ξ for t time steps while starting anywhere in $\mathcal{X}_{q_D}^0$. Given such reachable sets, it suffices to check if there exists a finite horizon H_{q_D} and at least one controller $\xi \in \Xi_{q_D \rightarrow q'_D}$ such that the reachable sets satisfy the following two conditions: (i) $\mathfrak{R}_t(\mathcal{X}_{q_D}^0, \xi) \subseteq \mathcal{X}_{q_D \rightarrow q_D}, \forall t \in [0, \dots, H_{q_D} - 1]$ and (ii) $\mathfrak{R}_{H_{q_D}}(\mathcal{X}_{q_D}^0, \xi) \subseteq \mathcal{X}_{q_D \rightarrow q'_D}$. If both conditions hold, we verify that the DFA transition from q_D to q'_D is *safe* given the initial set of states $\mathcal{X}_{q_D}^0$ and the controller ξ [6].

Construction of exact reachable sets is computationally intractable. Thus, instead, we compute over-approximated reachable sets, denoted hereafter by $\bar{\mathfrak{R}}_t(\mathcal{X}_{q_D}^0, \xi) \subseteq \mathfrak{R}_t(\mathcal{X}_{q_D}^0, \xi)$, using tools that can handle systems of the form (1) with NN controllers [8]. If the following two conditions are satisfied

$$\bar{\mathfrak{R}}_t(\mathcal{X}_{q_D}^0, \xi) \subseteq \mathcal{X}_{q_D \rightarrow q_D}, \forall t \in [0, \dots, H_{q_D} - 1] \quad (5)$$

$$\bar{\mathfrak{R}}_{H_{q_D}}(\mathcal{X}_{q_D}^0, \xi) \subseteq \mathcal{X}_{q_D \rightarrow q'_D}, \quad (6)$$

then we say that the considered DFA transition is *verified to be safe* given the initial set of states $\mathcal{X}_{q_D}^0$ and a feedback NN controller ξ .² Finally, if there is no self-loop for q_D , then $\mathcal{X}_{q_D \rightarrow q_D}$ cannot be defined. In this case, such a transition from q_D to q'_D is *verified to be safe* if (6) holds for $H_{q_D} = 1$.

Example 3.3 (Verifying Reach-Avoid Properties (cont)): Consider the DFA in Fig. 1a and, specifically, the transition from q_D^0 to q_D^1 . To reach q_D^1 from q_D^0 , the available controllers are $\Xi_{q_D^0 \rightarrow q_D^1} = \{\xi_1\}$ by construction of the set

¹In case $\mathcal{X}_{q_D \rightarrow q'_D}$ does not contain any region ℓ_i , then $\Xi_{q_D \rightarrow q'_D} = \emptyset$ by definition of Ξ ; see Ex. 3.3.

²In practice, reachable sets over a large enough horizon \bar{H} are computed. If there is not reachable set $\bar{\mathfrak{R}}_t$, for some $t \in \{0, \dots, \bar{H}\}$ that satisfies (6), then we say that the system fails to reach this region of interest. This is in accordance with related works; see e.g., [6], [8].

$\mathcal{X}_{q_D^0 \rightarrow q_D^1}$; see Ex. 3.2 and Section II. Let $\mathcal{X}_{q_D^0}^0 = \mathcal{X}_0$. Then, we compute reachable sets $\bar{\mathfrak{R}}_t(\mathcal{X}_0, \xi_1)$; see Fig. 1b. Observe that $H_{q_D^0} = 3$, since the sets $\bar{\mathfrak{R}}_t(\mathcal{X}_0, \xi_1)$ for $t = 0, 1, 2$ satisfy (5) and $\bar{\mathfrak{R}}_3(\mathcal{X}_0, \xi_1)$ satisfies (6). Thus, the transition from q_D^0 to q_D^1 is verified to be safe. For the transition from q_D^1 to q_D^F , we have that $\Xi_{q_D^1 \rightarrow q_D^F} = \{\xi_2\}$. Verification of this transition will be discussed in Ex. 3.4. Finally, we have $\Xi_{q_D^0 \rightarrow q_D^0} = \emptyset$ and $\Xi_{q_D^1 \rightarrow q_D^1} = \{\xi_1\}$.

D. From Verification of Reach-Avoid Properties to Verification of LTL formulas

To verify that the system satisfies ϕ , it suffices to check that the final DFA state can be reached from the initial state by enabling a sequence of DFA transitions that are verified to be safe; see also Section III-A. To check this we rely on applying graph-search methods over the DFA state while verifying on-the-fly safety of DFA transitions using reachability analysis; see Section III-C. Specifically, first we view the DFA as a directed graph $D = \{\mathcal{V}, \mathcal{E}\}$ with vertices \mathcal{V} and edges \mathcal{E} that are determined by the set of states and transitions of the DFA. As discussed in Section III-C, to verify safety of DFA transition, an initial set of states is needed denoted by $\mathcal{X}_{q_D}^0$. This set captures all possible states in \mathcal{X} that the system may have when it reaches a DFA state q_D . As a result, $\mathcal{X}_{q_D}^0$ depends on the previous DFA states that the system has gone through to reach q_D . To simplify the proposed algorithm, we pre-process D so that each node in D that can be reached through multiple paths (excluding self-loops) originating from q_D^0 is replicated so that each replica can be reached through a unique path (excluding self-loops). For each vertex $q_D \in \mathcal{V}$, we define sets that collect its incoming and outgoing edges denoted by $\mathcal{E}_{q_D}^{\text{in}}$ and $\mathcal{E}_{q_D}^{\text{out}}$, respectively. If the number of incoming edges (excluding self-loops) for q_D is greater than 1, i.e., $|\mathcal{E}_{q_D}^{\text{in}}| > 1$ we create $|\mathcal{E}_{q_D}^{\text{in}}|$ copies of q_D denoted by q_D^i . Each node q_D^i has only one incoming edge which is selected to be the i -th edge in $\mathcal{E}_{q_D}^{\text{in}}$, denoted by $\mathcal{E}_{q_D}^{\text{in}}(i)$, while its outgoing edges remain the same as in the original node q_D . Then we add all copies to the graph and remove the original nodes q_D . We denote the resulting graph by D' .

Next, we apply a Depth-first search (DFS) method over D' to see if q_D^F can be reached from q_D^0 through a sequence of DFA transitions that are verified to be safe. This process is summarized in Alg. 1. The inputs to this algorithm are the graph D' , the set Ξ of NN controllers and the system dynamics (1) (line 1). In what follows, we denote by q_D^{cur} the currently visited node in D' . The set of all possible states in \mathcal{X} that the system can be when it reaches q_D^{cur} is denoted by $\mathcal{X}_{q_D^{\text{cur}}}^0$. We initialize q_D^{cur} as $q_D^{\text{cur}} = q_D^0$ and $\mathcal{X}_{q_D^{\text{cur}}}^0 = \mathcal{X}_0$. Also, we define a set \mathcal{V}_{vis} that collects all nodes in D' that have been visited and a sequence \mathbf{q} of nodes that points to the current path from q_D^0 towards q_D^F . They are initialized as $\mathcal{V}_{\text{vis}} = \{q_D^0\}$ and $\mathbf{q} = q_D^0$. Also we initialize the control strategy ξ as an empty sequence. We also define a function $g : \mathcal{V} \rightarrow \mathcal{X}$ that maps a DFA state $q_D \in \mathcal{V}$ to the corresponding set $\mathcal{X}_{q_D}^0$; this function that is constructed on-the-fly is need only as way store and recover from memory the sets $\mathcal{X}_{q_D}^0$ (lines 2-

Algorithm 1 Reach_DFS Algorithm

```

1: Input:  $D'$ ; NN controllers  $\Xi$ ; System dynamics (1)
2: Output: Verification output  $R \in \{\text{True}, \xi, \text{False}\}$ 
3: Initialize  $q_D^{\text{cur}} \leftarrow q_D^0$ ;  $\mathcal{X}_{q_D^{\text{cur}}}^0 = \mathcal{X}_0$ ;  $\mathbf{q} = q_D^{\text{cur}}$ ;  $\mathcal{V}_{\text{vis}} = \{q_D^{\text{cur}}\}$ ;  $g(q_D^{\text{cur}}) \leftarrow \mathcal{X}_{q_D^{\text{cur}}}^0$ ;  $\xi \leftarrow \emptyset$ ;  $E = \text{False}$ ;
4: while  $E \neq \text{True}$  do
5:   Randomly select  $q_D^{\text{next}} \in \mathcal{R}_{q_D^{\text{cur}}}$ ;  $\mathcal{V}_{\text{vis}} \leftarrow \mathcal{V}_{\text{vis}} \cup q_D^{\text{next}}$ 
6:   Compute set of available controllers  $\Xi_{q_D^{\text{cur}} \rightarrow q_D^{\text{next}}}$ 
7:   if  $\exists H_{q_D^{\text{cur}}}$  and  $\xi \in \Xi_{q_D^{\text{cur}} \rightarrow q_D^{\text{next}}}$  for (5)-(6) then
8:      $\mathbf{q} = \mathbf{q} | q_D^{\text{cur}}$ ;  $\xi \leftarrow \xi | \xi$ ;  $\mathcal{X}_{q_D^{\text{next}}}^0 \leftarrow \bar{\mathfrak{R}}_{H_{q_D^{\text{cur}}}}(q_D^{\text{cur}})$ ;
9:      $q_D^{\text{cur}} \leftarrow q_D^{\text{next}}$ ;  $g(q_D^{\text{next}}) \leftarrow \mathcal{X}_{q_D^{\text{next}}}^0$ ;
10:    if  $q_D^{\text{cur}} = q_D^F$  then
11:       $R = [\text{True}, \xi]$ ;  $E = \text{True}$ ;
12:    else
13:       $\mathcal{R}_{q_D^{\text{cur}}} \leftarrow \mathcal{R}_{q_D^{\text{cur}}} \setminus q_D^{\text{next}}$ 
14:      while  $\mathcal{R}_{q_D^{\text{cur}}} \setminus \mathcal{V}_{\text{vis}} = \emptyset \wedge \mathbf{q} \neq \emptyset$  do
15:         $q_D^{\text{cur}} \leftarrow \mathbf{q}(\text{end})$ ;  $\mathcal{X}_{q_D^{\text{cur}}}^0 \leftarrow g(q_D^{\text{cur}})$ ;
16:         $\mathbf{q} \leftarrow \mathbf{q} \setminus \mathbf{q}(\text{end})$ ;  $\xi \leftarrow \xi \setminus \xi(\text{end})$ 
17:      if  $\mathcal{R}_{q_D^{\text{cur}}} \setminus \mathcal{V}_{\text{vis}} = \emptyset \wedge \mathbf{q} = \emptyset$  then
18:         $R \leftarrow \text{False}$ ;  $E \leftarrow \text{True}$ ;

```

3). Given q_D^{cur} , we randomly select a next state $q_D^{\text{next}} \in \mathcal{R}_{q_D^{\text{cur}}}$. Then we apply reachability analysis over the transition from q_D^{cur} to q_D^{next} using the NN controllers $\Xi_{q_D^{\text{cur}} \rightarrow q_D^{\text{next}}} \subseteq \Xi$ and the initial set of states $\mathcal{X}_{q_D^{\text{cur}}}^0$ (lines 5-6); see Section III-C. If the transition is verified to be safe, then we append q_D^{cur} to \mathbf{q} . Also, we append the controller $\xi \in \Xi_{q_D^{\text{cur}} \rightarrow q_D^{\text{next}}}$ for which this transition is safe to ξ that denotes the current control strategy to reach q_D^{next} from q_D^0 (lines 7-8). The corresponding horizon $H_{q_D^{\text{cur}}}$ should be stored as well; we abstain from this for simplicity of presentation. The final reachable set $\bar{\mathfrak{R}}_{H_{q_D^{\text{cur}}}}(q_D^{\text{cur}}, \xi)$ becomes the set $\mathcal{X}_{q_D^{\text{next}}}^0$; see Ex. 3.4 and Fig. 1b as well (line 8). Also, $g(q_D^{\text{next}})$ is constructed on-the-fly as $g(q_D^{\text{next}}) = \mathcal{X}_{q_D^{\text{next}}}^0$ and we replace q_D^{cur} with q_D^{next} (line 9). If the transition $q_D^{\text{cur}} \rightarrow q_D^{\text{next}}$ is not verified to be safe, we remove q_D^{next} from the set $\mathcal{R}_{q_D^{\text{cur}}}$ (see (3)). Then we keep taking out the last element in \mathbf{q} and ξ , denoted by $\mathbf{q}(\text{end})$ and $\xi(\text{end})$, while $\mathbf{q}(\text{end})$ is assigned to q_D^{cur} until we find another state in $\mathcal{R}_{q_D^{\text{cur}}}$ that has not been visited yet (lines 12-16). The above process is repeated until q_D^{cur} is updated to be q_D^F . In this case, we have found a NN control strategy ξ that satisfies ϕ for all initial states $\mathbf{x}_0 \in \mathcal{X}_0$ (line 10-11). If \mathbf{q} is empty yet we fail to find another state in $\mathcal{R}_{q_D^{\text{cur}}}$ that is not visited, then the proposed method cannot find a feasible path from q_D^0 to q_D^F (even though it may exist; see Section III-E) (lines 17-18). We note that any other graph-search method in conjunction with reachability analysis can be used as well.

Example 3.4 (LTL Verification (cont)): We continue Ex. 3.3; see also Fig. 1b. To verify the DFA transition from $q_D^{\text{cur}} = q_D^1$ to $q_D^{\text{next}} = q_D^F$, we initialize $\mathcal{X}_{q_D^1}^0 = \bar{\mathfrak{R}}_3(\mathcal{X}_0, \xi_1)$. By computing $\bar{\mathfrak{R}}_t(\mathcal{X}_{q_D^1}^0, \xi_2)$, we verify that this DFA transition is safe. Thus, there exists $\xi = \xi_1, \xi_2$ where ξ_1 and ξ_2 are applied for 3 and 2 time steps so that $f_\xi \models \phi$, for all $\mathbf{x}_0 \in \mathcal{X}_0$.

E. Correctness & Completeness

Proposition 3.5 (Correctness): The proposed method is correct, i.e., the computed ξ solves Problem 1.

Proof: This result holds by construction of the proposed

method. Particularly, we ensure that the closed-loop system (2) driven by $\xi = \mu(0), \dots, \mu(K)$, where each $\mu(k)$ is applied for H_k time-steps, generates trajectories $\tau(\mathbf{x}_0) = \mathbf{x}_0, \dots, \mathbf{x}_F$, where $F = \sum_{t=0}^{H_k}$, that satisfy the system dynamics and the LTL formula $\phi, \forall \mathbf{x}_0 \in \mathcal{X}_0$. ■

Remark 3.6 (Computational Efficiency vs Completeness):

In general, our method is not complete in the sense that it may not find a control strategy ξ that satisfies ϕ , for all $\mathbf{x}_0 \in \mathcal{X}_0$, even though such a strategy exists. This is due to the fact that (a) Alg. 1 computes over-approximated reachable sets and that (b) it does not exhaustively search over all possible combinations of NN control actions that the system can apply when a new DFA state is reached. As for (b), for instance, given a initial set of states for q_D^{cur} , Alg. 1 reasons about safety of a transition from q_D^{cur} to q_D^{next} , using only controllers selected from $\Xi_{q_D^{\text{cur}} \rightarrow q_D^{\text{next}}}$. If this transition is unsafe, then it is discarded. However, this transition may become feasible if the initial set of states changes, which can happen by applying a controller from $\Xi_{q_D^{\text{cur}} \rightarrow q_D^{\text{cur}}}$ for some \hat{H} time steps. Additionally, as soon as Alg. 1 finds a $\xi \in \Xi_{q_D^{\text{cur}} \rightarrow q_D^{\text{next}}}$ for which the corresponding transition is safe, it proceeds to new DFA transitions. However, that transition may be safe for other controllers in $\xi \in \Xi_{q_D^{\text{cur}} \rightarrow q_D^{\text{next}}}$ as well, where each one yields a different initial set for subsequent DFA transitions affecting their safety. The proposed method can be extended to account for these additional control actions at the expense of increasing its computational cost. We note that such trade-offs are quite common in related works; see e.g., [25]. The proposed method is complete if (i) there are no self-loops in the DFA states, or if $\Xi_{q_D \rightarrow q_D} = \emptyset$ for all states (see e.g., Ex. 3.3); (ii) $|\Xi_{q_D \rightarrow q_D^F}| = 1$, for all $q_D \in \mathcal{Q}_D \setminus \{q_D^F\}$; (iii) the reachable sets are accurately computed.

IV. EXPERIMENTS

In this section, we demonstrate our framework on an unmanned aerial vehicle (UAV) with various LTL properties.

System Dynamics: We consider a UAV with dynamics as in (1) where the matrices $\mathbf{A}_t, \mathbf{B}_t$, and \mathbf{c}_t are defined as in [8]. The UAV state is defined as $\mathbf{x} = [p_x; p_y; p_z; v_x; v_y; v_z] \in \mathbb{R}^6$ capturing the position and velocity. The control input $\mathbf{u} \in \mathbb{R}^3$ is a function of pitch, roll and thrust.

NN controllers: In what follows, we define LTL specifications that require the UAV to visit certain disjoint regions of interest $\ell_i \in \mathbb{R}^3$. We highlight that the the regions ℓ_i are defined only over the UAV position, i.e., $\ell_i \subseteq \Omega$. Also, since we assume disjoint regions, the DFA can be pruned by removing infeasible DFA transitions reducing the computational cost for verification [20]. We train the NN controllers similarly to [8]; nevertheless, any other method (e.g., RL) can be used to train them. Specifically, to train ξ_i , we leverage nonlinear Model Predictive Control (MPC) methods. First we generate a random set of states $\mathbf{x} \in \mathbb{R}^6$. Starting from each one of these states, we generate a sequence of pairs of states and control inputs that drive the UAV towards the interior of ℓ_i using an off-the-shelf MPC solver [26]. Each pair constitutes a data point in a training dataset. Using this dataset we train feedforward NN controllers ξ_i with 2 hidden

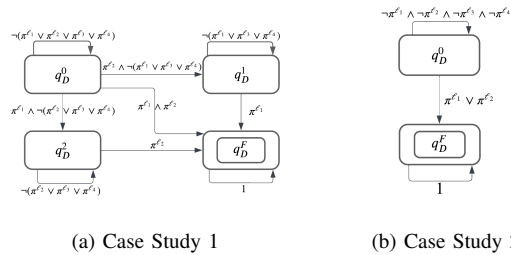


Fig. 2: DFA for the LTL formulas in case studies I & II.

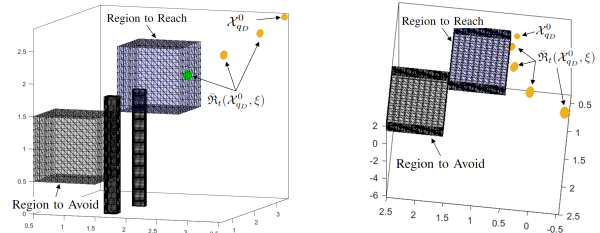


Fig. 3: Verification of a DFA transition for the case studies I & II. The regions of interest that need to be avoided/reached to enable this DFA transition are shown with black/blue colour. All other regions are not shown. All reachable sets that are outside/inside the regions to reach are shown with orange/green color.

layers, 30 neurons/layer, and ReLU activation functions.

Case Study I: In this case study, we consider the following LTL formula $\phi = (\diamond \pi^{\ell_1}) \wedge (\diamond \pi^{\ell_2}) \wedge (\neg(\pi^{\ell_3} \vee \pi^{\ell_4}) \mathcal{U} \pi^{\ell_1}) \wedge (\neg(\pi^{\ell_3} \vee \pi^{\ell_4}) \mathcal{U} \pi^{\ell_2})$ requiring the UAV to eventually visit the regions ℓ_1 and ℓ_2 , in any order, while avoiding the obstacles ℓ_3 and ℓ_4 . This formula corresponds to the DFA shown in Fig. 2a; notice that the transition from q_D^0 to q_D^F was pruned and, therefore, not considered during verification since it requires the UAV to be present in more than one region simultaneously. To train ξ_1 and ξ_2 we collected 16000 data-points for each controller. Given these trained NN controllers and an initial set \mathcal{X}_0 of states defined as an ellipsoid centered at $[3.5; 3.5; 2.9]$ with shape matrix of $\text{diag}[0.5^2; 0.5^2; 0.5^2]$. We check if there exists a sequence of control actions that satisfy ϕ . Particularly, first it investigates the DFA transition from q_D^0 to q_D^1 . This transition requires the UAV to stay within the obstacle-free space (i.e., avoid the obstacles ℓ_3 and ℓ_4) and eventually reach ℓ_2 . The corresponding reachable sets for this DFA transition are shown in Figure 3a. Notice that the reachable sets $\bar{\mathfrak{R}}_t(\mathcal{X}_0, \xi_2)$ are fully outside the obstacle regions for $t = 1, 2$ while at $t = 3$ the corresponding reachable set is fully inside ℓ_2 . Thus, this DFA transition is verified to be safe. Next, the DFA transition from q_D^1 to q_D^F is considered requiring the robot to reach ℓ_1 while avoiding the obstacle regions. The set of initial states for this transition is $\mathcal{X}_{q_D^1}^0 = \bar{\mathfrak{R}}_3(\mathcal{X}_0, \xi_2)$. After computing reachable sets $\bar{\mathfrak{R}}_t(\mathcal{X}_{q_D^1}^0, \xi_1)$ (not shown), we can see that for $t = 1, 2$ they are outside the obstacles while $\bar{\mathfrak{R}}_3(\mathcal{X}_{q_D^1}^0, \xi_1)$ is inside ℓ_1 verifying that this DFA transition is also safe. Thus, there exists a control strategy $\xi = \xi_2, \xi_1$ where $H_1 = H_2 = 3$ such that $\mathbf{f}_\xi \models \phi$ for all $\mathbf{x}_0 \in \mathcal{X}_0$.

Case Study II: In this case study, we consider an LTL formula $\phi = \diamond(\pi^{\ell_1} \vee \pi^{\ell_2}) \wedge (\neg(\pi^{\ell_3} \vee \pi^{\ell_4}) \mathcal{U}(\pi^{\ell_1} \vee \pi^{\ell_2}))$

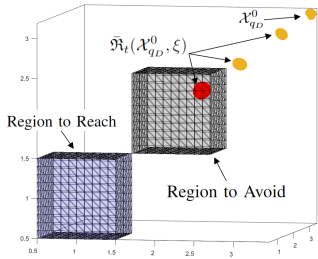


Fig. 4: Case Study III: Verification of the DFA transition from q_D^0 to q_D^1 . The red ellipsoid corresponds to a reachable set being fully inside the region to avoid.

requiring the UAV to eventually visit either region ℓ_1 or ℓ_2 , while avoiding obstacles ℓ_3 and ℓ_4 . This formula corresponds to the DFA shown in Figure 2b. The NN controller ξ_2 is the same as in the previous case study while ξ_1 was trained using only 100 datapoints to mimic a poorly designed controller. The initial set of states \mathcal{X}_0 is defined as an ellipsoid centered at $[0.4; 0.4; 0.3]$ with shape matrix of $\text{diag}[0.5^2; 0.5^2; 0.5^2]$. Given the DFA, we investigate the transition from q_D^0 to q_D^F which requires the UAV to reach either ℓ_1 or ℓ_2 while avoiding both ℓ_3 and ℓ_4 . In other words, we have that $\mathcal{X}_{q_D^0 \rightarrow q_D^0} = \{\Omega \setminus (\ell_3 \cup \ell_4)\}$ and $\mathcal{X}_{q_D^0 \rightarrow q_D^F} = \{\ell_1 \cup \ell_2\}$. Thus, we have that $\Xi_{q_D^0 \rightarrow q_D^F} = \{\xi_1, \xi_2\}$. First, we check if this DFA transition is safe using ξ_1 . The generated reachable sets are shown in Figure 3b; only the first 4 reachable sets are shown. We observed that ℓ_1 could not be reached within a large enough number of iterations. Thus, we cannot reason about safety of this DFA transition under ξ_1 . Thus, next we consider the controller ξ_2 and we constructed the sets $\mathfrak{R}_t(\mathcal{X}_0, \xi_2)$ (not shown) demonstrating that all obstacles are avoided while at $t = 6$ the the reachable set is fully inside ℓ_2 . Thus, we verify that there exists $\xi = \xi_2$, where ξ_2 is applied for 6 steps, so that $\mathbf{f}_\xi \models \phi$, for all $\mathbf{x}_0 \in \mathcal{X}_0$.

Case Study III: We revisit the LTL formula considered in Ex. 3.2-3.4 with DFA shown in Fig. 1a. The controllers ξ_1 and ξ_2 are the same as in case study I while \mathcal{X}_0 is defined as an ellipsoid centered at $[3.4; 3.4; 3.1]$ with shape matrix of $\text{diag}[0.5^2; 0.5^2; 0.5^2]$. To check whether the DFA transition from q_D^0 to q_D^1 is safe, we check if the system can reach ℓ_1 while avoiding ℓ_2 . By constructing the reachable sets, we notice that ℓ_1 cannot be reached without entering ℓ_2 first; see Fig. 4. Thus, we cannot find a ξ for ϕ ; see Rem. 3.6.

V. CONCLUSION

This paper proposed a new method to design verified compositions of NN controllers for co-safe LTL tasks. We showed its efficiency in navigation tasks for aerial vehicles.

REFERENCES

- [1] Q. Gao, D. Hajinezhad, Y. Zhang, Y. Kantaros, and M. M. Zavlanos, "Reduced variance deep reinforcement learning with temporal logic specifications," in *10th ACM/IEEE International Conference on Cyber-Physical Systems*, 2019, pp. 237–248.
- [2] V. Rubies-Royo, D. Fridovich-Keil, S. Herbert, and C. J. Tomlin, "A classification-based approach for approximate reachability," in *2019 International Conference on Robotics and Automation (ICRA)*. IEEE, 2019, pp. 7697–7704.
- [3] S. Huang, N. Papernot, I. Goodfellow, Y. Duan, and P. Abbeel, "Adversarial attacks on neural network policies," *arXiv preprint arXiv:1702.02284*, 2017.
- [4] M. Fazlyab, M. Morari, and G. J. Pappas, "Safety verification and robustness analysis of neural networks via quadratic constraints and semidefinite programming," *IEEE Trans on Automatic Control*, 2020.

- [5] S. Dutta, S. Jha, S. Sankaranarayanan, and A. Tiwari, "Output range analysis for deep feedforward neural networks," in *NASA Formal Methods Symposium*. Springer, 2018, pp. 121–138.
- [6] C. Huang, J. Fan, W. Li, X. Chen, and Q. Zhu, "Reachnn: Reachability analysis of neural-network controlled systems," *ACM Transactions on Embedded Computing Systems (TECS)*, vol. 18, no. 5s, pp. 1–22, 2019.
- [7] X. Sun, H. Khedr, and Y. Shoukry, "Formal verification of neural network controlled autonomous systems," in *International Conference on Hybrid Systems: Computation and Control*, 2019, pp. 147–156.
- [8] H. Hu, M. Fazlyab, M. Morari, and G. J. Pappas, "Reach-sdp: Reachability analysis of closed-loop systems with neural network controllers via semidefinite programming," *59th IEEE Conference on Decision and Control (CDC)*, pp. 5929–5934, December 2020.
- [9] H.-D. Tran, X. Yang, D. M. Lopez, P. Musau, L. V. Nguyen, W. Xiang, S. Bak, and T. T. Johnson, "NNV: The neural network verification tool for deep neural networks and learning-enabled cyber-physical systems," *Computer Aided Verification*, vol. 12224, pp. 3–17, 2020.
- [10] S. Dutta, X. Chen, and S. Sankaranarayanan, "Reachability analysis for neural feedback systems using regressive polynomial rule inference," in *Proceedings of the 22nd ACM International Conference on Hybrid Systems: Computation and Control*, 2019, pp. 157–168.
- [11] R. Ivanov, T. Carpenter, J. Weimer, R. Alur, G. Pappas, and I. Lee, "Verisig 2.0: Verification of neural network controllers using taylor model preconditioning," in *International Conference on Computer Aided Verification*. Springer, 2021, pp. 249–262.
- [12] S. Sun, Y. Zhang, X. Luo, P. Vlantis, M. Pajic, and M. M. Zavlanos, "Formal verification of stochastic systems with relu neural network controllers," in *2022 International Conference on Robotics and Automation (ICRA)*. IEEE, 2022, pp. 6800–6806.
- [13] K. Jothimurugan, S. Bansal, O. Bastani, and R. Alur, "Compositional reinforcement learning from logical specifications," *Advances in Neural Information Processing Systems*, vol. 34, 2021.
- [14] G. N. Tasse, D. Jarvis, S. James, and B. Rosman, "Skill machines: Temporal logic composition in reinforcement learning," *arXiv preprint arXiv:2205.12532*, 2022.
- [15] C. Neary, C. Verginis, M. Cubuktepe, and U. Topcu, "Verifiable and compositional reinforcement learning systems," in *Proceedings of the International Conference on Automated Planning and Scheduling*, vol. 32, 2022, pp. 615–623.
- [16] R. Ivanov, K. Jothimurugan, S. Hsu, S. Vaidya, R. Alur, and O. Bastani, "Compositional learning and verification of neural network controllers," *ACM Trans. Embed. Comput. Syst.*, vol. 20, no. 5s, sep 2021. [Online]. Available: <https://doi.org/10.1145/3477023>
- [17] C. Baier and J.-P. Katoen, *Principles of model checking*. MIT press Cambridge, 2008, vol. 26202649.
- [18] S. W. Chen, T. Wang, N. Atanasov, V. Kumar, and M. Morari, "Large scale model predictive control with neural networks and primal active sets," *Automatica*, vol. 135, p. 109947, 2022.
- [19] K. Leahy, D. Zhou, C.-I. Vasile, K. Oikonomopoulos, M. Schwager, and C. Belta, "Persistent surveillance for unmanned aerial vehicles subject to charging and temporal logic constraints," *Autonomous Robots*, vol. 40, no. 8, pp. 1363–1378, 2016.
- [20] Y. Kantaros and M. M. Zavlanos, "Stylus*: A temporal logic optimal control synthesis algorithm for large-scale multi-robot systems," *International Journal of Robotics Research*, 2020.
- [21] E. M. Hahn, M. Perez, S. Schewe, F. Somenzi, A. Trivedi, and D. Wojtczak, "Omega-regular objectives in model-free reinforcement learning," *TACAS*, 2018.
- [22] Y. Kantaros, "Accelerated reinforcement learning for temporal logic control objectives," in *IEEE/RSJ International Conference on Intelligent Robots and Systems*, Kyoto, Japan, October 2022.
- [23] A. K. Bozkurt, Y. Wang, M. M. Zavlanos, and M. Pajic, "Control synthesis from linear temporal logic specifications using model-free reinforcement learning," in *2020 IEEE International Conference on Robotics and Automation (ICRA)*. IEEE, 2020, pp. 10 349–10 355.
- [24] F. Fuggitti, "Ltlf2dfa," March 2019. [Online]. Available: <https://github.com/whitemech/LTLf2DFA>
- [25] K. Leahy, A. Jones, and C. I. Vasile, "Fast decomposition of temporal logic specifications for heterogeneous teams," *IEEE Robotics and Automation Letters*, 2022.
- [26] N. Andrei, "A sqp algorithm for large-scale constrained optimization: Snoop," in *Continuous nonlinear optimization for engineering applications in GAMS technology*. Springer, 2017, pp. 317–330.